Clim Dyn (2012) 39:1169–1181
DOI 10.1007/s00382-012-1334-z

# Revisiting Asian monsoon formation and change associated with Tibetan Plateau forcing: I. Formation

**Guoxiong Wu · Yimin Liu · Buwen Dong · Xiaoyun Liang · Anmin Duan · Qing Bao · Jingjing Yu**

Received: 1 August 2011 / Accepted: 7 March 2012 / Published online: 5 April 2012


**Abstract** Numerical experiments with different idealized land and mountain distributions are carried out to study the formation of the Asian monsoon and related coupling processes. Results demonstrate that when there is only extratropical continent located between 0 and 120°E and between 20/30°N and the North Pole, a rather weak monsoon rainband appears along the southern border of the continent, coexisting with an intense intertropical convergence zone (ITCZ). The continuous ITCZ surrounds the whole globe, prohibits the development of near-surface cross-equatorial flow, and collects water vapor from tropical oceans, resulting in very weak monsoon rainfall. When tropical lands are integrated, the ITCZ over the longitude domain where the extratropical continent exists disappears as a consequence of the development of a strong surface cross-equatorial flow from the winter hemisphere to the summer hemisphere. In addition, an intense interaction between the two hemispheres develops, tropical water vapor is transported to the subtropics by the enhanced poleward flow, and a prototype of the Asian monsoon appears. The Tibetan Plateau acts to enhance the coupling between the lower and upper tropospheric circulations and between the subtropical and tropical monsoon circulations, resulting in an intensification of the East Asian summer monsoon and a weakening of the South Asian summer monsoon. Linking the Iranian Plateau to the Tibetan Plateau substantially reduces the precipitation over Africa and increases the precipitation over the Arabian Sea and the northern Indian subcontinent, effectively contributing to the development of the South Asian summer monsoon.

**Keywords** Rainfall pattern · Tibetan Plateau thermal forcing · Positive feedback mechanism · Vorticity balance · Global warming

This paper is a contribution to the special issue on Global Monsoon Climate, a product of the Global Monsoon Working Group of the Past Global Changes (PAGES) project, coordinated by Pinxian Wang, Bin Wang, and Thorsten Kiefer.

G. Wu · Y. Liu (✉) · A. Duan · Q. Bao
State Key Laboratory of Numerical Modeling for Atmospheric Sciences and Geophysical Fluid Dynamics,
Institute of Atmospheric Physics,
Chinese Academy of Sciences, Beijing, China
e-mail: lym@lasg.iap.ac.cn

B. Dong
Department of Meteorology, National Centre for Atmospheric Science, University of Reading, Reading, UK

X. Liang
National Climate Center,
China Meteorological Administration, Beijing, China

J. Yu
National Meteorological Information Center,
China Meteorological Administration, Beijing, China

## 1 Introduction

The monsoon is generally considered an atmospheric response to the change in land-sea thermal contrast induced by the seasonal evolution of solar radiation (Wallace and Hobbs 1977; Holton, 2004). However, the monsoon is not controlled by simple land-sea thermal contrast alone; zonal asymmetric diabatic heating and large-scale orography can significantly affect it (e.g., Chen 2003; Wu et al. 2009; Kucharski et al. 2010). Wave–mean flow interaction is another method of fully understanding the dynamics of monsoon circulation. Schneider and Bordoni (2008) showed that over the course of seasonal cycles simulated with an idealized general circulation model (GCM) without

a hydrological cycle and with a uniform lower boundary, the Hadley cell undergoes rapid transitions between the eddy-dominated regime around the equinoxes and a more closely angular momentum–conserving regime around the solstices. Bordoni and Schneider (2008) used reanalysis data to show that the onset of the Asian monsoon marks a transition between the two circulation regimes. Further study from Bordoni and Schneider (2010) suggests that in axisymmetric steady-state simulations, the strength of the cross-equatorial Hadley cell, the location and intensity of the main convergence zone, and the upper- and lower-level winds in the summer subtropics do not change as rapidly as in the corresponding eddy-permitting simulations.

Using the post-First Global Atmospheric Research Program (GARP) Global Experiment (FGGE) data and horizontal dimension fitting to the monsoon circulation, Chen (2003) proposed a planetary-scale perspective on the maintenance of summer monsoon circulations and illustrated some basic features common to the major monsoon circulations in Asia, North America, South America, and Australia that differ from the classic monsoon circulation model. He demonstrated that monsoon circulation is "driven by the east–west differential heating and maintained dynamically by a balance between a vorticity source and advection. This dynamic balance is reflected by a spatial quadrature relationship between the monsoon divergent circulation and the monsoon high (low) at upper (lower) levels." On the other hand, based on reanalysis-data diagnosis, Wu and Liu (2003) revealed a spatial quadrature relation between monsoon circulations and the vertical diabatic heating profile and reported that such a relation is a consequence of the land-sea distribution along the subtropics. They demonstrated that although in summer there is generally heating over the continent and cooling over the ocean, a quadrupole heating pattern exists over each subtropical continent and its adjacent oceans. The ocean region to the west of the continent is characterized by strong longwave radiative cooling (LO); the western and eastern portions of the quadrupole heating are dominated by sensible heating (SE) and condensation heating (CO), respectively; and the ocean region to the east of the continent is characterized by double dominant heating (D), with LO prevailing over CO. These then compose a LOSECOD heating quadrupole. Accompanying this LOSECOD heating pattern is a distinct circulation pattern: in the upper troposphere, anticyclonic circulation over the continent is accompanied by cyclonic circulations over the oceans on its western and eastern sides, while near the surface, cyclonic circulation over the continent is accompanied by anticyclonic circulations over the oceans on both sides. Liu et al. (2004) and Wu et al. (2009) further interpreted such a heating and circulation coupling by using the following Sverdrup balance of potential vorticity equation:

$$\beta v \approx \eta \theta_z^{-1} \partial Q/\partial z, \tag{1}$$

Where $\beta = \partial f/\partial y$, $\eta = f + \zeta$ is absolute vorticity, and $Q$ is diabatic heating; the other symbols are conventional notations in meteorology. They showed that across each subtropical continent, desert and monsoon are jointly formed as a twin system by large-scale continental forcing, local-scale sea-breeze forcing, and regional-scale orographic forcing. By defining a streamfunction $\psi$,

$$v = \partial\psi/\partial x$$

the explicit quadrature relation between the streamfunction and the diabatic heating profile can be obtained as follows:

$$\partial\psi/\partial x = \eta(\beta\theta_z)^{-1}\partial Q/\partial z. \tag{2}$$

As demonstrated in Wu and Liu (2003), a continental surface monsoon low is coupled with an upper tropospheric high and is accompanied by CO to its east and surface SE and radiation cooling to its west. Thus *a monsoon circulation is not simply "driven by the east–west differential heating"; rather it is associated with the east–west differential heating profile.*

Using general circulation model (AGCM) experiments, Kucharski et al. (2010) found that both north–south and east–west contrasts in atmospheric heating contributed to the maintenance of the South Asian summer monsoon (SASM), but their relative impact depended on regional scales: the monsoon circulation and precipitation over northern India are mainly due to the north–south contrast, whereas the low-level cyclone and rainfall in the Bay of Bengal and southern India result from the east–west gradient. Xu et al. (2009) examined the relative impacts of various land-sea distributions and mountains on the extent and intensity of the Asian monsoon by conducting a series of AGCM simulations. They found that the tropical subcontinental-scale zonal land-sea distribution and the Asian mountains contribute almost equally to the enhancement of the monsoon circulation and play a more important role than the large-scale meridional land-sea contrast between the Eurasian continent and the Indian Ocean.

In addition to land-sea thermal contrast, the shape and location of the continent can affect monsoon circulation as well. Chou (2003) employed an intermediate atmospheric model coupled with a mixed-layer ocean and simple land-surface model having an idealized Afro-Eurasian continent but no physical topography in order to study how the tropospheric temperature gradient induced by land-sea distribution and Tibetan Plateau (TP) forcing affects the intensity of the Asian summer monsoon. It was shown that an increase in prescribed heating and a weaker surface

albedo over Eurasia and the TP can strengthen the meridional temperature gradient, enhance the Asian summer monsoon circulation, and favor strong convection. Chou (2003) thus concluded that "the corresponding monsoon rainbelt extends northward and northeastward". This agrees well with the observation that in association with the weakening trend in the surface sensible heat flux over the TP during the past several decades, the Asian summer monsoon circulation has also weakened, leading to flooding in southern China and drought in northern China (Duan and Wu 2008, 2009; Yang et al. 2011). Based on conceptual land distribution, Young (1987) and Dirmeyer (1998) reported that the latitude of a continent could influence the surface flow, and the location and shape of the land can affect monsoon climate. However, the land used in Young's study was a simple rectangle; the northern boundary of the land used in Dirmeyer's experiments extended to only 40°N. Consequently, a false forcing associated with artificial baroclinic instability is imposed on the atmosphere near the northern boundary of the continent, resulting in an annually persistent rainfall maximum occurring at midlatitudes rather than at low latitudes, particularly in summer. In addition, the size of the mountain in Dirmeyer's experiments is comparable to the continent, which may also unfavorably affect the underlying physics.

To further understand the influence of land-sea distribution and large-scale orography on the Asian monsoon, we performed a series of aqua-planet experiments based on a GCM by using various idealized land distributions similar to those of Chou (2003) and Liang et al. (2006), but focusing on their influences on tropical-subtropical coupling, the coupling between the Southern and Northern hemispheres, and the coupling between the lower and upper troposphere, as these couplings can influence the configuration and intensity of the monsoon. These idealized land-sea distribution experiments are complementary to the recent study of Kucharski et al. (2010), which focused on understanding the role of the north–south and east–west thermal contrasts in the SASM. In addition, the influence of large-scale orography on the formation of the Asian monsoon system is also investigated by embedding into the continent an idealized TP as well as Iranian Plateau (IR) and diagnosing their dynamic and thermal influences compared with those from the experiments without orographic forcing.

The model employed for this study and the experiment design are introduced in Sect. 2. The influence of an extratropical continent alone on atmospheric circulation is examined in Sect. 3; the coexistence of an intertropical convergence zone (ITCZ) and a monsoon rainband is also demonstrated. The contribution of the integration of a tropical subcontinent and an extratropical continent to the formation of a prototype Asian monsoon is discussed in Sect. 4. The development of the East Asian monsoon (EAM) due to the existence of the TP is discussed in Sect. 5. In Sect. 6, an idealized IR is connected to the TP, and its effect of blocking cold and dry airflow from the north on the development of the South Asian monsoon (SAM) is analyzed. A summary and conclusions are presented in Sect. 7.

## 2 Model description and experiment design

The numerical model used for this study is the spectral AGCM developed at the State Key Laboratory of Numerical Modeling for Atmospheric Sciences and Geophysical Fluid Dynamics, Institute of Atmospheric Physics (IAP/LASG). This model has nine levels in the vertical and is rhomboidally truncated at wave-number 42 in the horizontal (i.e., the SAMIL-R42L9 version; Wu et al. 2003). The Simplified Simple Biosphere model SSiB (Xue et al. 1991) has been used to calculate land surface processes (Liu and Wu 1997). This model can simulate the observed climatology well, including sea level pressure, precipitation, specific humidity, geopotential high, temperature, and winds (Wu et al. 2003). To conduct sensitivity experiments, the entire surface of the model Earth is first covered with water to form an aqua-planet experiment (Exp AQU), as demonstrated in the Aqua-Planet Experiment Project (Chapter 4.16, APE, http://www.met.reading.ac.uk/~mike/APE/atlas.html). The sea surface temperature (SST) used in all experiments is the zonally averaged climatological SST provided by the Second Atmospheric Model Intercomparison Program (AMIP-II, Fiorino 2000), which has seasonal variation. Consequently, the tropical east–west thermal contrast that existed in Kucharski et al. (2010) is absent at the initial state. The zonal mean of the model climatology of wind, temperature, humidity, and surface pressure from Exp AQU are taken as initial values for other idealized experiments.

Five types of land distributions with different geometries are embedded in the aqua-planet for different experiments (Table 1). In Exp MID, a continent is located over 0°–120°E and 30°–90°N to investigate the influence of a continent at middle and high latitudes on circulations. In Exp SUB, the southern boundary of the continent in Exp MID is extended 10° southward into the subtropics, mimicking the main part of the Eurasian continent. In Exp TRO, three square-shaped tropical lands over (0°–50°E, 35°S–20°N), (75°–85°E, 5°–20°N), and (95°–105°E, 9°S–20°N) are introduced to represent the tropical African, Indian, and Indochina Peninsula subcontinents, respectively, which are then integrated into the main Eurasian continent as in Exp SUB to form the "Afro-Eurasian continent," as was done in our previous study (Liang et al. 2006). Exp TP uses

**Table 1** Experiment design in the idealized aqua-planet experiments

| Experiment | Distribution of land | Focus of the experiment |
|---|---|---|
| MID | Higher-latitude continent (0°–120°E, 30°–90°N) | Land-sea coupling; relation of monsoon with ITCZ |
| SUB | Subtropical continent (0°–120°E, 20°–90°N) | |
| TRO | Tropical continent (SUB land and 0°–50°E, 35°S–20°N; 75°–85°E, 5°–20°N; and 95°–105°E, 9°S–20°N) | Tropical-subtropical coupling; Interhemispheric coupling; relation of monsoon with ITCZ |
| TP | TRO and TP (TRO land and an elliptic topography with maximum altitude of 5,000 m, centered at 87.5°E, 32.5°N) | Tropical-subtropical coupling; Lower- and upper-troposphere coupling; development of EAM |
| TP-IR | TP and IR (TP and an elliptic topography IR with maximum altitude of 3,000 m, centered at 53.4°E, 32.5°N) | Effects of Iran Plateau on the development of SAM |

the same continent as that in Exp TRO, but adds an idealized TP to investigate its influence on the monsoon. Since the IR is comparable in size to the TP, another experiment, Exp TPIR, is designed, in which the idealized IR is added to Exp TP to investigate its impacts on the monsoon. Because the spin-up period of the model, as measured by the global mean surface air temperature, is about 6 months, all of these experiments were integrated for 10 years, and the means of the last 8 years were used for the following analyses.

## 3 Coexistence of ITCZ and monsoon-effect due to an extratropical continent

The distributions of rainfall and wind at the lowest model level $\sigma = 0.991$ in Exp MID are shown in Fig. 1a and b. In January (Fig. 1a), in addition to the equatorial rainfall along the ITCZ, the main precipitation at midlatitudes appears over the ocean. Strong northwesterly winds (>20 m $s^{-1}$) develop along the offshore region east of the continent in thermally adapting to the underlying warm SST (Wu and Liu 2000), which agrees with wintertime observations (Wu et al. 2009). Along the eastern front of the continental anticyclone, this strong northerly transports high potential vorticity from middle and high latitudes to the subtropics. Transient high-vorticity perturbations in the subtropics are then transported westward along the easterly, forming another band of apparent rainfall (4–6 mm $day^{-1}$) to the south of the continent, resembling the mechanism of zonally asymmetric instability (Hsu and Plumb 2000; Liu et al. 2007).

In July (Fig. 1b), continental heating generates a large-scale near-surface cyclone over land. Precipitation occurs along the southern and eastern boundaries of the continent in a seemingly monsoonlike distribution. However, unlike the Asian monsoon, in which the most intense rainfall appears over the southern and southeastern continent, in Exp MID the maximum rainfall appears over the ocean. The area enclosed by thick red curves in Fig. 1b denotes the region in which the change in wind direction exceeds 120°—one of the criteria proposed by Ramage (1971) in defining the monsoon. A large area with a change in wind direction exceeding 120° appears to the south of the continent between 20° and 30°N, where the January rainfall exceeds 4 mm $day^{-1}$, presenting a weak winter monsoon. Over the eastern continent, on the other hand, no significant change in wind direction or rainfall is observed, and therefore no summer monsoon over land is produced in Exp MID.

In Exp SUB, the subtropical land experiment, the southern boundary in Exp MID is extended to 20°N, close to the northern end of the Arabian Sea (ABS), the Bay of Bengal (BOB), and the South China Sea (SCS). The simulated January circulation at $\sigma = 0.991$ (Fig. 1c) is similar to that in Exp MID, with strong rainfall and northerly wind developing along 120°–135°E. However, these do not reach low latitudes, nor do they interact with the tropical easterly. Rainfall in the tropics is confined to the weak winter ITCZ. The simulated July circulation (Fig. 1d) is also similar to its counterpart in Exp MID (Fig. 1b). Weak rainfall (4–6 mm $day^{-1}$) occurs over the southeastern corner of the continent. A reversal in wind direction between January and July occurs along the southern boundary. The appearance of a seasonal wind reversal and weak rainfall over the southeastern continent indicates the occurrence of a "weak" East Asian summer monsoon (EASM) in Exp SUB.

Despite their differences, the simulated climates in Exps MID and SUB bear some prominent common features. First, the weak "monsoon" near the southern continental boundary and the ITCZ along the equator coexist as two distinct entities where the continent exists (0°–120°E). Consequently, there is no apparent transequatorial flow from one hemisphere to another in either winter or summer. Second, these two rainbands in summer are associated with a near-surface westerly in the north and a tropical easterly to the south, respectively, while the area of zonal-wind transition in between experiences rare rainfall. To aid in understanding these similarities, Fig. 2a and c show the meridional circulations in these two experiments. Figure 2a shows the ocean domain between 150° and 180°E in Exp

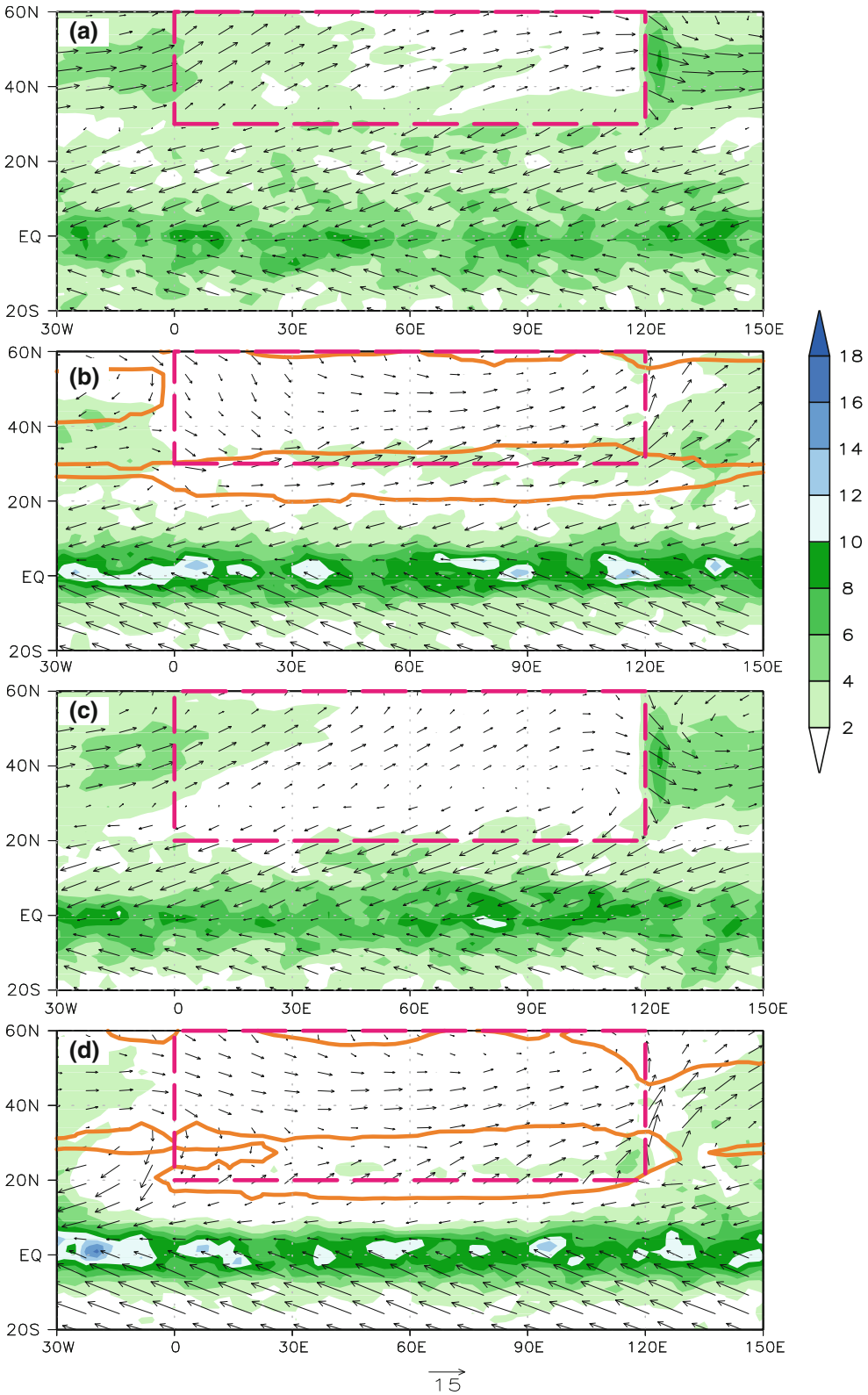


**Fig. 1** Wind vectors at $\sigma = 0.991$ (*arrows*; the unit vector shown at the *bottom* of the figure is in m $s^{-1}$) and precipitation (*shading*; in mm $day^{-1}$) in January (**a** and **c**) and July (**b** and **d**) in Exps MID (**a** and **b**) and SUB (**c** and **d**). The areas enclosed by *thick orange lines* in (**b**) and (**d**) denote regions where the difference in wind direction between January and July exceeds 120°. The heavy *dashed line* denotes the continent boundary

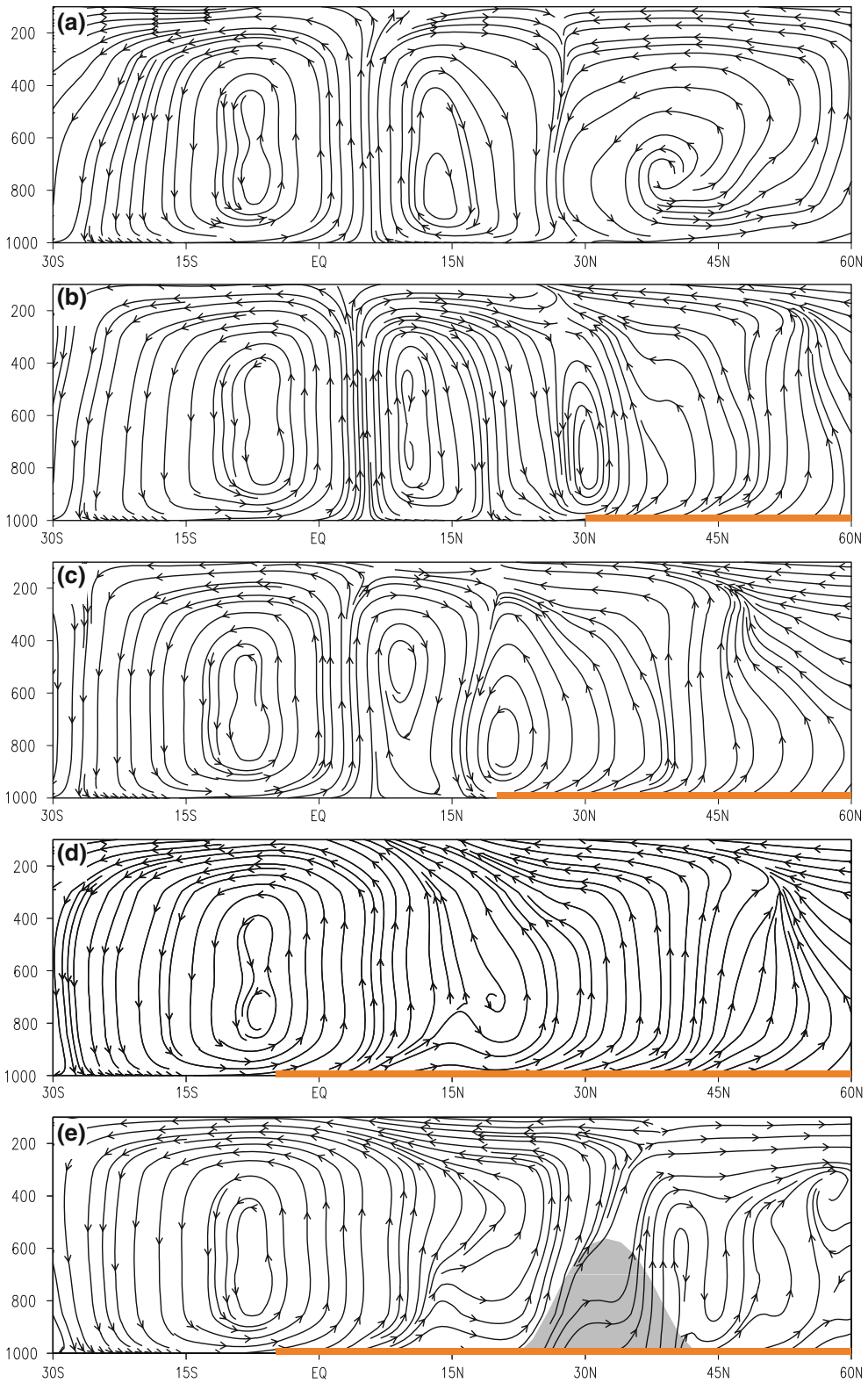


**Fig. 2** July mean meridional circulation averaged over the ocean domain between 150°E and the dateline in Exp SUB (**a**) and over the eastern continent domain between 90° and 120°E in Exps MID (**b**), SUB (**c**), TRO (**d**), and TPIR (**e**). The *solid colored lines* at the *bottom* of (**b**) through (**e**) indicate where the continent is located in the corresponding experiment, and the shading in (**e**) denotes the TP shape across 87.5°E

SUB, representing the mean meridional circulation. The corresponding meridional circulation in Exp MID is similar (not shown). Figure 2b and c show the eastern continent domain averaged between 90° and 120°E in Exps MID and SUB, respectively. In all three panels (Fig. 2a–c) there is no significant difference in the Southern Hemisphere meridional circulation. In the Northern Hemisphere over the ocean, a complete thermally direct cell in the tropics between 5° and 30°N and an indirect cell at midlatitudes between 30° and 60°N are pronounced (Fig. 2a). A significant difference exists over the continent. The persistent land heating in summer generates dominant ascending air over the eastern part of the continent, which induces a "monsoon type" of meridional circulation with an ascending arm over land in the north and a descending arm over the ocean in the south, forming a center just above the southern edge of the continent (Fig. 2b, c). As a result, the meridional extent of the "Hadley cell" decreases the farther the continent penetrates equatorward-farther south in Exp SUB than in Exp MID. Consequently, the descending arm of the Hadley cell is centered near 25°N in Exp MID and near 15°N in Exp SUB, corresponding to the "dry" belts in Fig. 1b and d.

The ITCZ between the Northern Hemisphere and Southern Hemisphere Hadley cells maintains a continuous convection belt surrounding the globe near the equator (Fig. 1). This suppresses water vapor transport across the equator. Furthermore, a substantial portion of the water vapor over the tropical ocean converges toward the ITCZ to form heavy rainfall; only a minor part is left to sustain the "monsoon" to the north. The monsoon rainfall therefore becomes rather weak in both winter and summer. This implies that when the monsoon rain belt and the ITCZ coexist in the same longitude domain, the monsoon intensity will become weaker. In addition, in Exp MID, the water vapor that is transported to sustain the monsoon is from a wider belt of the tropical ocean south of 30°N, whereas in Exp SUB it is from a narrower belt south of 20°N. Thus, the "monsoon rainfall" in Exp MID is apparently stronger than that in Exp SUB in both winter and summer.

## 4 Rudiments of the Asian monsoon—the influence of tropical land

In Exp TRO, in which three pieces of tropical land are introduced and connected to the subtropical land, the distributions of rainfall and circulation at high latitudes (Fig. 3) show insignificant change compared with those in Exp SUB (Fig. 1). However, marked changes are evident in the tropics. In January (Fig. 3a), a strong northeasterly sweeps from the subtropical continent to the tropics before it crosses the equator to the Southern Hemisphere. The ITCZ rainband produces more rain over the land and less over the ocean. In July (Fig. 3b), a southwesterly monsoon develops over South and East Asia from the tropics to the subtropics. Cross-equatorial flow from the Southern Hemisphere brings a large amount of moisture to sustain the Asian monsoon. The continuous ITCZ in Exps MID and SUB (Fig. 1) is now broken into segments. The rain belt over Africa and the Indian Ocean is pushed northward; the rain belt over South and Southeast Asia tilts northwest-southeast to form a "monsoon trough"; only the rain belt over the Pacific remains along the ITCZ. A wind reversal between winter and summer occurs over a vast area in the subtropics and tropics, similar to the observed Asian monsoon.

To further investigate the influence of tropical land-sea distribution on tropical-subtropical coupling and inter-hemisphere coupling, as well as on the Asian monsoon, the differences in rainfall and circulation at $\sigma = 0.991$ between Exps TRO and SUB are analyzed. In January (Fig. 3c), the introduction of tropical land generates cross-equatorial flow from the Northern Hemisphere, particularly over Africa and the western Indian Ocean, contributing to the intensification of rainfall in the Southern Hemisphere. In July (Fig. 3d), the tropical land introduction results in a marked intensification of the southwesterly in the tropics and the cross-equatorial flow from the Southern Hemisphere. The rain belt over the Asian sector is shifted northward from along the equatorial ITCZ by about 15°, forming a broad and intense monsoon rain belt between 5°N and 20°N, extending from Africa to the SCS. Rainfall over South Asia occurs mainly within the southwesterly, representing part of the southwesterly Asian monsoon rainfall rather than the ITCZ rainfall. The southwesterly also transfers a large amount of moisture from the tropics to the subtropics, enhancing the "East Asian monsoon" by pushing the rainband farther northward.

Figure 2d shows the meridional circulation in July averaged between 90° and 120°E in Exp TRO. It is characterized by ascending air over the land and descending air over the ocean. The extension of the extratropical continent into the tropics thus results in the disruption of the northern thermally direct (Hadley) cell, which exists in Exps MID and SUB (Fig. 2b, c). As the ITCZ over the tropical land regions disappears, the strong southerly originating from the Southern Hemisphere tropics crosses the equator and penetrates into the continent, contributing to the enhancement of the Asian monsoon. In other words, the existence of tropical land promotes interaction between the two hemispheres and between the tropics and subtropics in the Northern Hemisphere. Note that in this experiment with only an idealized land-sea distribution, the EAM already exists, though it is weaker than observations, with a

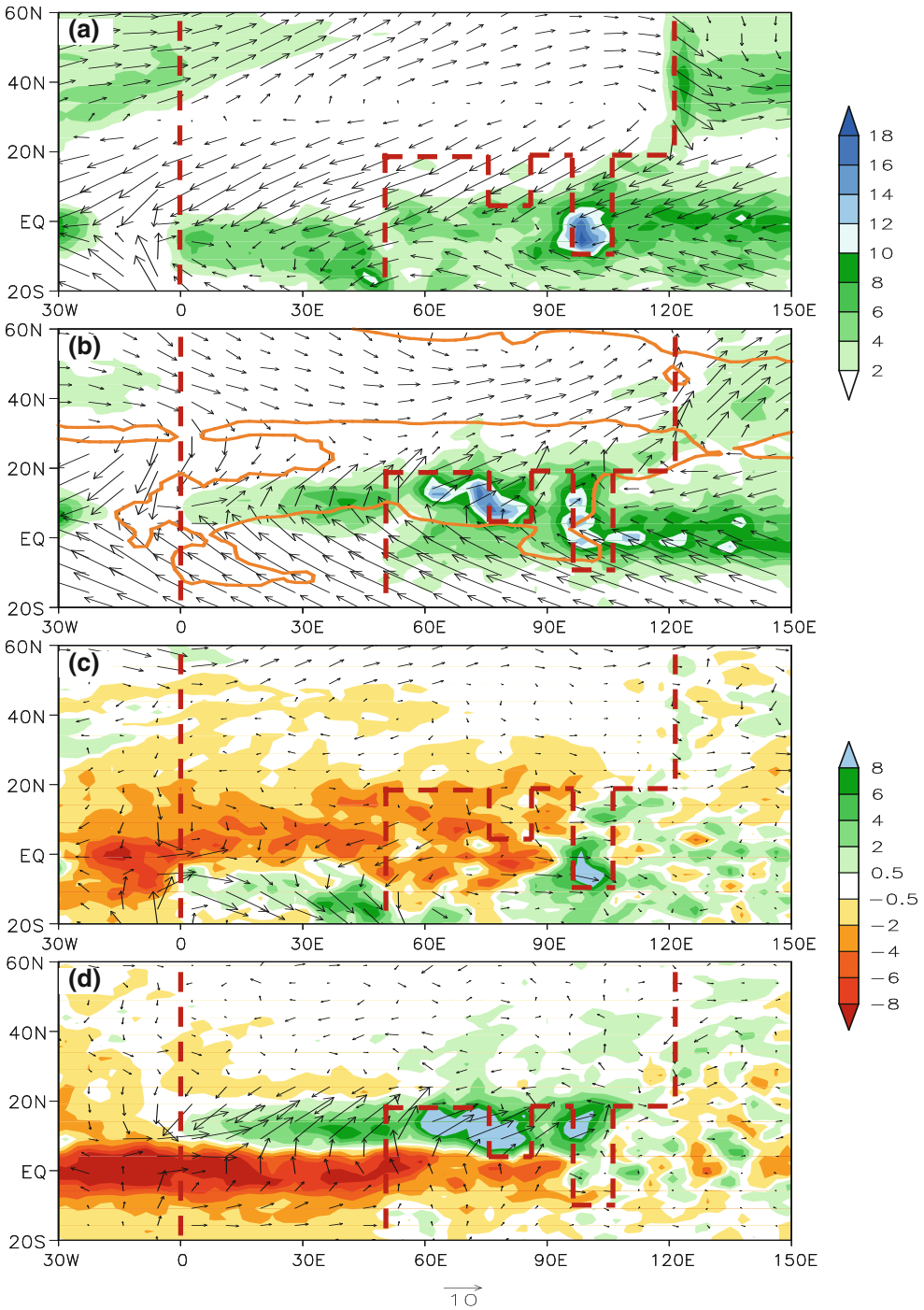


**Fig. 3** Distributions of wind vectors at $\sigma = 0.991$ (*arrows*; the unit vector shown at the *bottom* of the figure is in m $s^{-1}$) and precipitation (shading; in mm $day^{-1}$) in Exp TRO (**a** and **b**) and the differences between Exps TRO and SUB (**c** and **d**) in January (**a** and **c**) and July (**b** and **d**). The areas enclosed by *thick red lines* in (**b**) denote regions where the difference in wind direction between January and July exceeds 120°. The *heavy dashed line* denotes the continent boundary

maximum of 4–6 mm $day^{-1}$ confined to a small region in the southeastern corner of the continent (Fig. 3b), even without the presence of the TP.

Although no east–west thermal gradient exists at the initial stage of Exp TRO, the rainfall configuration in Fig. 3b indicates a CO associated with a southerly over the southeastern continent and a SE and radiative cooling associated with a northerly over the western continent along the tropical-subtropical areas. Correspondingly, a monsoon low exists over the land and subtropical highs occur over the oceans. Eventually, a Sverdrup balance in (1) and (2) is developed between the east–west gradient of

the heating profile and the monsoon circulation in the tropical and subtropical areas. Because the rainfall pattern in Fig. 3b resembles the observed Asian summer monsoon to some extent, we may infer that land-sea distribution, especially that across South Asia, plays a fundamental role in the formation of a prototype Asian monsoon, particularly its southern portion.

## 5 Development of the east Asian monsoon—the influence of the Tibetan Plateau

It has long been recognized that heating over the TP can affect the Asian monsoon (e.g., Yeh et al. 1957; Flohn 1957; Ye and Wu 1998; Liu and Yin 2002; Yanai and Wu 2006; Wu et al. 2007, 2009). Such heating generates a lower-level cyclonic circulation in the surrounding area and an upper-level anticyclone aloft, pumping the warm, moist surface air from the surrounding area to the upper troposphere over its eastern portion. To further investigate the underlying dynamics, an idealized TP with the following ellipsoidal shape is placed on the continent in Exp TRO:

$$h(\lambda,\varphi) = h_{\max} \cdot \cos\left(\frac{\pi}{2}\frac{\lambda-\lambda_0}{\lambda_d}\right)\cos\left(\frac{\pi}{2}\frac{\varphi-\varphi_0}{\varphi_d}\right)$$

where $(\lambda_0, \varphi_0)$ denotes the longitude and latitude of the TP center, $h_{\max}$ is its maximum height, and $(\lambda_d, \varphi_d)$ is its half-width in longitude and latitude. In Exp TP $(\lambda_0, \varphi_0)$, $(\lambda_d, \varphi_d)$, and $h_{\max}$ are taken as (87.5°E, 32.5°N), (25°, 8.25°), and 5 km, respectively. The ellipse presented in Fig. 4a and b denotes the contour $h(\lambda, \phi) = 1,000$ m.

Figure 4a shows the simulated distributions of precipitation and the wind field in July at the near-surface level $\sigma = 0.991$ in Exp TP. Figure 4b shows the differences between the experiments with and without the TP, i.e., between Figs. 4a and 3b. The elevated mountain heating produces not only lower-troposphere cyclonic circulation but also strong rainfall (>16 mm $d^{-1}$) on the southeastern slope of the TP, partly because the local SE generates a geostrophic Rossby wave that ascends to the east and descends to the west, and partly because over the southeastern TP the upstream warm, moist air which is transported along the southwesterly from the Indian Ocean is pumped upward.

The large-scale latent heating associated with this strong rainfall induces a Gill-type Rossby wave circulation (Gill 1980), with a northerly of >5 m $s^{-1}$ to its west and an intense southerly of >10 m $s^{-1}$ to its east and southeast (Fig. 4a). The difference between Exps TP and TRO as presented in Fig. 4b reveals that the existence of the TP enhances the subtropical anticyclone over the western North Pacific, increases the rainfall over the BOB, eastern TP, and eastern Asia, while it decreases the rainfall over central Asia, the Arabian Sea, and the Indian subcontinent. The relatively unified tropical-subtropical coupling, as presented in Exp TRO (Fig. 3b), is thus deformed to become a regional pattern: increased rainfall to the east and decreased rainfall to the west. This is because the introduction of the TP induces positive feedback processes in the Asian monsoon region, as explained next.

When the zonal flow is weak, the potential vorticity equation at a steady state can be approximated by the Sverdrup relation, as presented in (1). Because the latent heating associated with the condensation of water vapor carried by the southerly increases with height in the lower troposphere, following (1), it produces positive vorticity. For a quasi–steady state, this generation of positive vorticity should be balanced by the negative planetary vorticity advection of the southerly. The development of the southerly provides more water vapor to sustain the convective instability and thus the monsoon rainfall. Therefore, the generation of positive vorticity and the monsoon latent heating form a positive feedback via development of the southerly. Consequently, we infer that it is the intensification of the southerly due to the existence of the TP that enhances the coupling between the tropics and subtropics and between the two hemispheres, resulting in the strong development of the subtropical East Asian monsoon.

The strong northerly to the west of the circulation transports cold, dry air southward from the subtropics toward central Asia, the Arabian Sea, and India, thereby strongly reducing the summer rainfall there. Because diffusive SE decreases with increasing height, Eq. (1) indicates that negative vorticity is produced. To maintain a steady state, positive planetary vorticity transfer is required via a northerly from higher latitudes, which would continuously bring cold air from the north and, in return, further enhance surface SE. Thus, via the meridional transfer of vorticity and energy, a quasi–steady state is maintained by surface SE and the prevailing northerly to the west of the TP. Furthermore, the development of a persistent dry northerly in these areas causes continuous surface evaporation. Consequently, a rainfall reduction area appears over central Asia, the Arabian Sea, and India, as shown in Fig. 4b, implying that an isolated TP alone will weaken the SASM.

The above results obtained from Exp TP are basically the same as those obtained in Liang et al. (2006); however, Exp TP uses an updated version of the numerical model. In this run, the heavy rainfall appears mainly over the southeastern TP and to its east, while rainfall over northern and western India is weak in the simulation (Fig. 4a). The decreased Indian rainfall due to the introduction of the TP as shown in Fig. 4b contradicts the general notion that increased TP forcing results in enhanced Indian rainfall

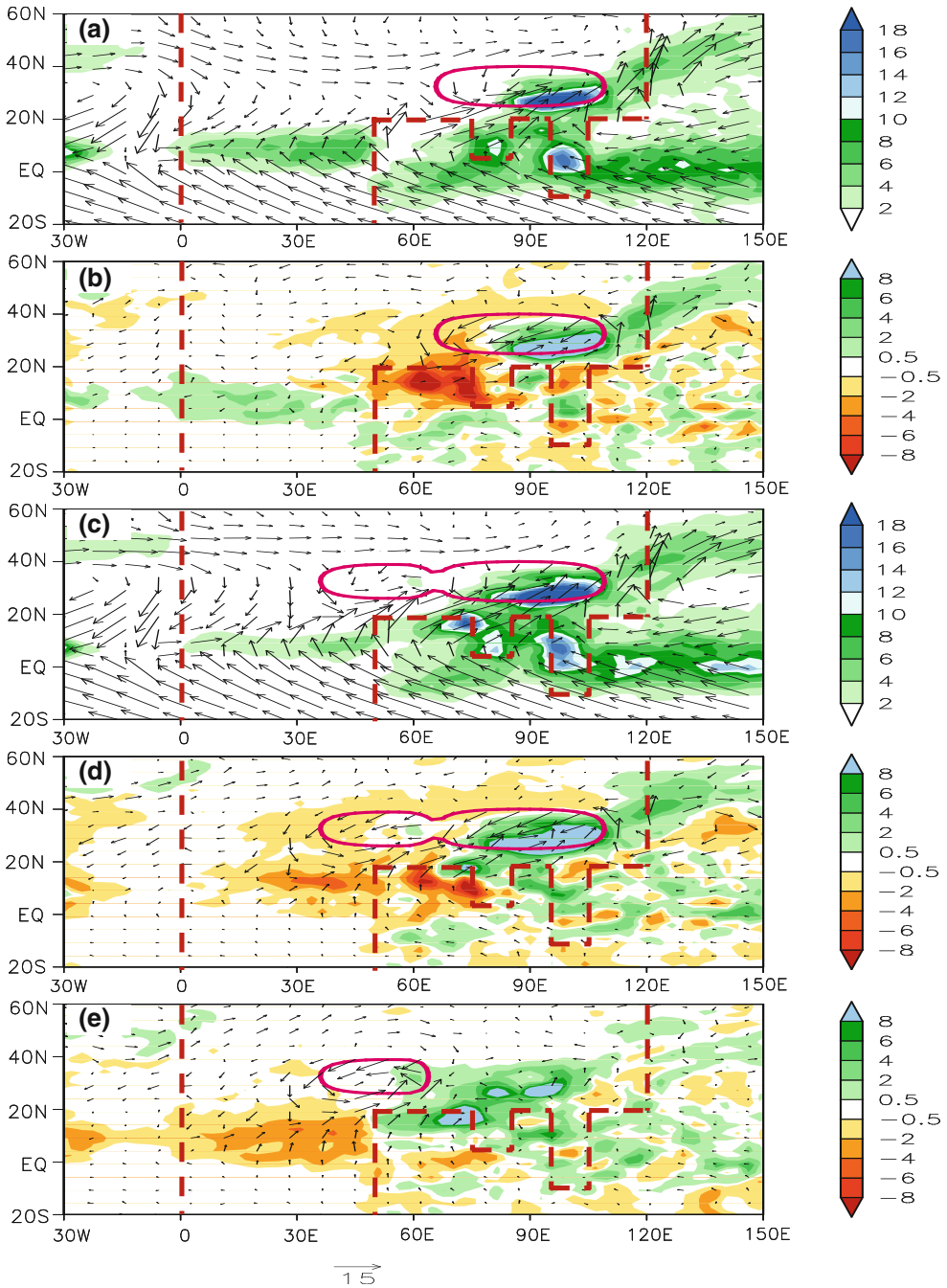


**Fig. 4** Wind vectors at $\sigma = 0.991$ (*arrows*; the unit vector shown at the *bottom* of the figure is in m $s^{-1}$) and precipitation (*shading*; in mm $day^{-1}$) in July in Exp TP (**a**); difference between Exps TP and TRO (**b**); Exp TPIR (**c**); difference between Exps TPIR and TRO (**d**); and difference between Exps TPIR and TP (**e**). The *heavy curve* denotes the orographic contour at 700 m, and the *heavy dashed line* denotes the continent boundary. [Refer to Fig. 10 in Wu et al. (2009) and Fig. 6 in Liang et al. (2006).]

(e.g., Duan et al. 2006). It also contradicts the correlation analysis result that stronger/weaker TP forcing in summer corresponds to increased/decreased precipitation over northern India, as we will see in Part II of this study.

To understand the above mentioned discrepancy from observations, we explore the impact of the "Iranian Plateau" next.

## 6 Development of the South Asian monsoon-blocking effect of the Iranian Plateau

In reality, there is another plateau, the IR, which is the same size as the TP and located to the west of it. So a new experiment is designed, in which both the "Iranian Plateau" and the "Tibetan Plateau" are present to explore the

discrepancy mentioned in Sect. 5. To mimic the impacts of the IR together with the TP, an orography similar to the TP but with different parameters of $(\lambda_0, \varphi_0)$, $(\lambda_d, \varphi_d)$, and $h_{\max}$ set at (53.4°E, 32.5°N), (22.5°, 8.25°), and 3 km, respectively, is added to Exp TP, and this is Exp TPIR.

Figure 4c is similar to Fig. 4a but represents Exp TPIR. Compared to Exp TP, dramatic changes occur over South Asia: a rainfall area of more than 10 mm day$^{-1}$ appears, with a center of about 16 mm day$^{-1}$ over its northwestern offshore region. The weakened South Asian monsoon in Exp TP is overcome in Exp TPIR. The difference between Exps TPIR and TRO as presented in Fig. 4d shows that the existence of the TP and IR not only enhances the EAM but also shifts the South Asian rainband northward and contributes to the formation of the northern branch of the Indian monsoon.

Figure 4e shows the difference between Fig. 4c and a, representing the contribution of the IR to the development of the South Asian monsoon. The IR forcing induces a near-surface cyclonic circulation. The anomalous northerly to its west reduces the rainfall over North Africa. On the contrary, the anomalous southerly to its east cancels the northerly that exists in Exp TP (Fig. 4a) and brings water vapor to sustain the rainfall over the area from the eastern Arabian Sea to southeastern Asia, forming a rain belt mimicking the SASM. We may infer that the presence of the IR generates a strong southerly to its east and southeast and blocks the cold and dry northerly from the north that exists only if the TP orographic forcing is imposed (as in Exp TP), thus contributing to the formation of the South Asian monsoon, at least to its northern part.

Figure 5 shows the meridional cross sections of meridional wind v and vertical velocity $(-\omega \cdot 60)$ averaged between 90° and 120°E for Exp TPIR (a), Exp TRO (b), and their differences (c). After the mountain ranges of the TP and IR are introduced, the southerly from the tropics to the

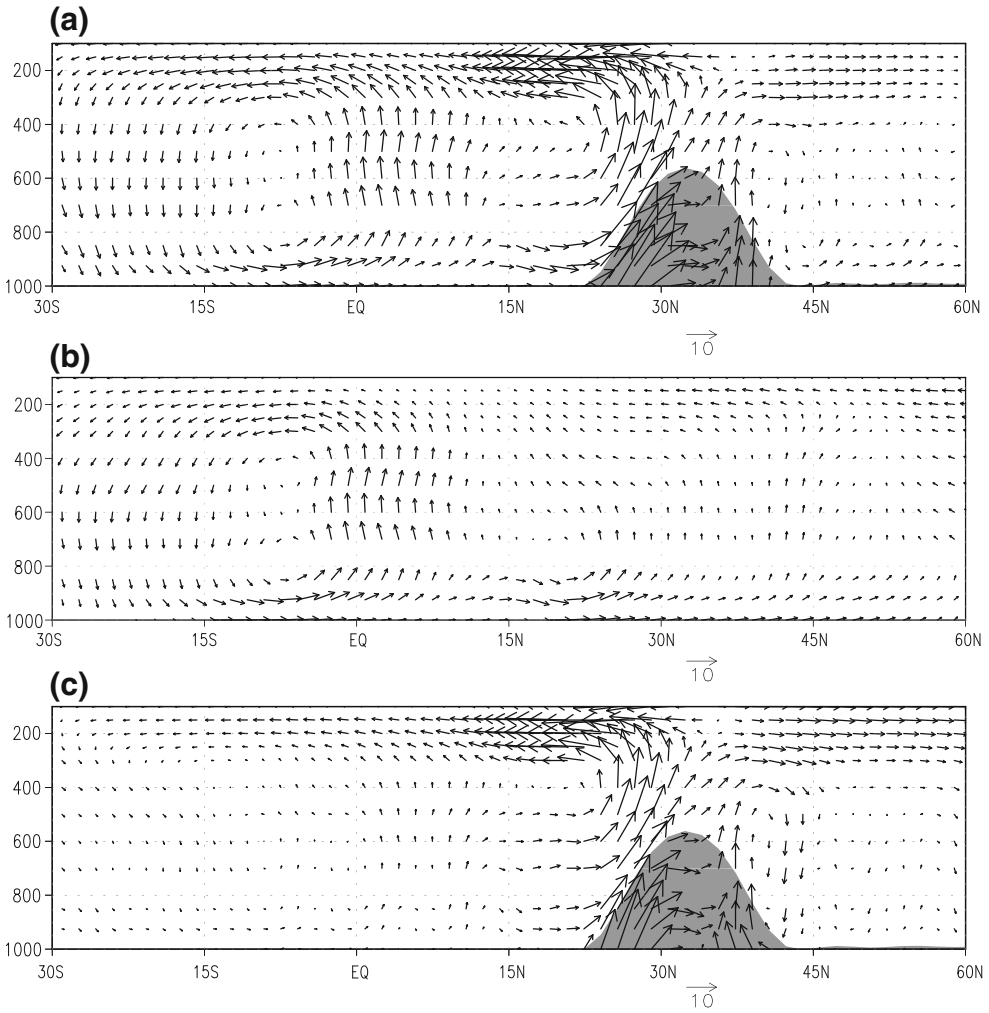


**Fig. 5** Mean meridional circulation (v, $-\omega$) averaged over the eastern continent domain between 90° and 120°E in Exps TPIR (**a**), TRO (**b**), and their difference (**c**). The *shading* in (**a**) and (**c**) denotes the TP shape across 87.5°E. The vertical pressure velocity $\omega$ is amplified by 60 in the plotting

subtropics and the upward motion over the southern slope of the TP are substantially increased. This implies that large-scale orography plays a significant role in enhancing the circulation coupling between the tropics and subtropics, and between the lower and upper troposphere. The marked intensification of the coupling between the tropics and subtropics causes a large amount of moisture to be transported to higher latitudes from tropical regions (Fig. 5a, c). Consequently, the July rainband over East China is pushed farther northward, and about 2–4 mm day$^{-1}$ more rainfall occurs over northern China, Korea, and northern Japan.

## 7 Summary

Although seasonal changes in land-sea thermal contrast that result from the annual evolution of the solar azimuth are essential for the occurrence of the monsoon, the idealized experiments presented in this study reveal that these seasonal changes alone are not a sufficient condition for the existence of the monsoon. For a continent located at extratropical latitudes, the experiments (Exps MID and SUB) produce seasonal changes in land-sea thermal contrast but give insignificant monsoon rainfall. In such circumstances, a very weak monsoon rainband coexists with the ITCZ along the equator, and tropical water vapor substantially converges to the ITCZ, which effectively prohibits the interaction of circulation systems between the two hemispheres.

The existence of tropical land creates an asymmetric thermal contrast between the two hemispheres. Cross-equator flows in winter and summer thus develop, and the zonal symmetry of the ITCZ in Exps MID and SUB is destroyed. Abundant water vapor evaporated from the tropical oceans in the Northern and Southern hemispheres is transported from the winter hemisphere to the summer hemisphere to sustain the remarkable precipitation in the summer hemisphere's tropical area. The occurrence of heavy precipitation and wind reversal between winter and summer in this area marks the formation of a prototype Asian monsoon. It is obvious that the tropical land plays an essential role in enhancing the circulation coupling between the Southern and Northern hemispheres.

The uplifted orographic thermal forcing in summer generates a cyclonic circulation in the lower troposphere, with a southerly to its east and a northerly to its west. Consequently, TP forcing strengthens the circulation coupling between the subtropics and tropics, and between the lower and upper troposphere. Abundant water vapor is transported from the tropical ocean to the extratropical continent to its east, where it condenses during the course of northward travel, thereby developing a strengthened EAM. The integration of the IR into the TP generates an extra cyclonic circulation in the lower troposphere, which contributes to the dryness in North Africa and the occurrence of heavy precipitation over the Arabian Sea and northern India. This, together with the forcing induced by the tropical land, causes the South Asian monsoon to develop.

In this study, the prescribed SST is zonally averaged, which excludes the east–west thermal contrast induced by SST. The Asian monsoon system develops as a consequence of land-sea distribution and large-scale mountains. These results do not rule out the contributions of the east–west gradient of either diabatic heating or the heating profile to the development of the Asian monsoon. Indeed, as tropical land and large-scale mountains are introduced into the integration, strong rainfall occurs over the eastern continent, and thus the east–west thermal contrast develops during the course of this simulation. The east–west thermal contrast and monsoon circulations interact with each other during monsoon development and eventually reach a Sverdrup balance, as presented in (1). In this regard, large-scale mountains and land-sea distribution could be considered the primary forcing factors of the monsoon climate.

**Acknowledgments** This study was jointly supported by the MOST Programme (2010CB950403 and 2012CB417200), and the NSFC Projects (40925015, 40875034). BD was supported by the U.K. National Centre for Atmospheric Science-Climate (NCAS-Climate). We thank the anonymous reviewers for their valuable suggestions on the improvement of the manuscript.

## References

Bordoni S, Schneider T (2008) Monsoons as eddy-mediated regime transitions of the tropical overturning circulation. Nat Geosci 1:515–519. doi:10.1038/ngeo248

Bordoni S, Schneider T (2010) Regime transitions of steady and time-dependent hadley circulations: comparison of axisymmetric and eddy-permitting simulations. J Atmos Sci 67:1643–1654

Chen TC (2003) Maintenance of summer monsoon circulations: a planetary-scale perspective. J Clim 16(12):2022–2037 doi:10.1175/1520-0442(2003)016<2022:MOSMCA>2.0.CO;2

Chou C (2003) Land-sea heating contrast in an idealized Asian summer monsoon. Clim Dyn 21(1):11–25. doi:10.1007/s00382-003-0315-7

Dirmeyer PA (1998) Land-sea geometry and its effect on monsoon circulations. J Geophys Res 103(D10)(10):11555–11572. doi:10.1029/98JD00802

Duan AM, Wu GX (2008) Weakening trend in the atmospheric heating source over the Tibetan Plateau during recend decades. Part I: observations. J Clim 21:3150–3164

Duan AM, Wu GX (2009) Weakening trend in the atmospheric heating source over the Tibetan Plateau during recend decades. Part II: connection with climate warming. J Clim 22:4197–4212

Duan K, Yao T, Thompson LG (2006) Response of monsoon precipitation in the Himalayas to global warming. J Geophys Res 111(19D19):D19110. doi:10.1029/2006JD007084

Fiorino M (2000) AMIP II sea surface temperature and sea ice concentration observations. PCMDI Report, Lawrence Livermore National Laboratory

Flohn H (1957) Large-scale aspects of the "summer monsoon" in South and East Asia. J Meteorol Soc Jpn 75:180–186

Gill AE (1980) Some simple solutions for heat-induced tropical circulation. Q J Roy Meteor Soc 106(449):447–662. doi:10.1002/qj.49710644905

Holton JR (2004) An introduction to dynamic meteorology. Elsevier Academic Press, Amsterdam, p 535

Hsu CJ, Plumb RA (2000) Nonaxisymmetric thermally driven circulations and upper-tropospheric monsoon dynamics. J Atmos Sci 57(9):1255–1276. doi:10.1175/1520-0469(2000)057<1255:NTDCAU>2.0.CO;2

Kucharski F, Bracco A, Barimalala R, Yoo JH (2010) Contribution of the east-west thermal heating contrast to the South Asian monsoon and consequences for its variability. Clim Dyn 37:721–735. doi:10.1007/s00382-010-0858-3

Liang XY, Liu YM, Wu GX (2006) Roles of tropical and subtropical land-sea distribution and the Qinghai-Xizang Plateau in the formation of the Asian summer monsoon. Chin J Geophys-Ch 49(4):983–992 (in Chinese)

Liu H, Wu GX (1997) Impacts of land surface on climate of July and onset of summer monsoon: a study with an AGCM plus SSiB. Adv Atmo- spheric Sci 14:289–308

Liu X, Yin ZY (2002) Sensitivity of East Asian monsoon climate to the uplift of the Tibetan Plateau. Palaeogeogr Palaeocl 183(3–4):223–245. doi:10.1016/S0031-0182(01)00488-6

Liu Y, Wu G, Ren R (2004) Relationship between the subtropical anticyclone and diabatic heating. J Clim 17(4):682–698. doi:10.1175/1520-0442(2004)017<0682:RBTSAA>2.0.CO;2

Liu Y, Hoskins B, Blackburn M (2007) Impact of the Tibetan orography and heating on the summer flow over Asia. J Meteorol Soc Jpn 85B:1–19. doi:10.2151/jmsj.85B.1

Ramage CS (1971) Monsoon meteorology. Academic Press, New York, p 296

Schneider T, Bordoni S (2008) Eddy-mediated regime transitions in the seasonal cycle of a Hadley circulation and implications for monsoon dynamics. J Atmos Sci 65:915–934

Wallace JM, Hobbs PV (1977) Atmospheric Science: an introductory survey. Academic Press, New York

Wu G, Liu Y (2000) Thermal adaptation, overshooting, dispersion, and subtropical anticyclone Part I: Thermal adaptation and overshooting. Chin J Atmos Sci 24(4):433–446 (in Chinese). doi:10.3878/j.issn.1006-9895.2000.04.01

Wu G, Liu Y (2003) Summertime quadruplet heating pattern in the subtropics and the associated atmospheric circulation. Geophys Res Lett 30(5):1201. doi:10.1029/2002GL016209

Wu T, Liu P, Wang Z, Liu Y, Yu R, Wu G (2003) The performance of atmospheric component model R42L9 of GOALS/LASG. Adv Atmos Sci 20(5):726–742. doi:10.1007/BF02915398

Wu G, Liu Y, Wang T, Wan R, Liu X, Li W, Wang Z, Zhang Q, Duan A, Liang X (2007) The influence of the mechanical and thermal forcing of the Tibetan Plateau on the Asian climate. J Hydrometeorl 8(4):770–789. doi:10.1175/JHM609.1

Wu GX, Liu Y, Zhu X, Li W, Ren R, Duan A, Liang X (2009) Multi-scale forcing and the formation of subtropical desert and monsoon. Ann Geophys 27(9):3631–3644. doi:10.5194/angeo-27-3631-2009

Xu Z, Fu C, Qian Y (2009) Relative roles of land-sea distribution and orography in Asian monsoon intensity. J Atmos Sci 66(9):2714–2729

Xue Y, Sellers PJ, Kinter JJ, Shukla J (1991) A simplified biosphere model for global climate studies. J Clim 4:345–364

Yanai M, Wu GX (2006) Effects of the Tibetan Plateau. In: Wang B (ed) The Asian monsoon. Springer, Berlin, pp 513–549. doi:10.1007/3-540-37722-0_13

Yang K, Guo XF, He J, Qin J, Koike T (2011) On the climatology and trend of the atmospheric heat source over the Tibetan Plateau: An experiments-supported revisit. J Clim 24:1525–1541

Ye DZ, Wu GX (1998) The role of the heat source of the Tibetan Plateau in the general circulation. Meteorol Atmos Phys 67(1–4):181–198. doi:10.1007/BF01277509

Yeh TC, Lo SW, Chu PC (1957) The wind structure and heat balance in the lower troposphere over Tibetan Plateau and its surrounding. Acta Meteor Sinica 28:108–121 (in Chinese)

Young JA (1987) Physics of monsoon: the current view. In: Fein JS, Stephens PL (eds) Monsoons. Wiley, Washington D C, pp 211–243